

## Proposal for Quantum Simulation via All-Optically-Generated Tensor Network States

I. Dhand,<sup>1,2</sup> M. Engelkemeier,<sup>3</sup> L. Sansoni,<sup>3</sup> S. Barkhofen,<sup>3</sup> C. Silberhorn,<sup>3</sup> and M. B. Plenio<sup>1,2</sup>

<sup>1</sup>*Institut für Theoretische Physik, Albert-Einstein-Allee 11, Universität Ulm, 89069 Ulm, Germany*

<sup>2</sup>*Center for Integrated Quantum Science and Technology (IQST), Albert-Einstein-Allee 11, Universität Ulm, 89069 Ulm, Germany*

<sup>3</sup>*Department of Physics and CeOPP, University of Paderborn, Warburger Strasse 100, D-33098 Paderborn, Germany*

 (Received 26 October 2017; revised manuscript received 16 January 2018; published 27 March 2018)

We devise an all-optical scheme for the generation of entangled multimode photonic states encoded in temporal modes of light. The scheme employs a nonlinear down-conversion process in an optical loop to generate one- and higher-dimensional tensor network states of light. We illustrate the principle with the generation of two different classes of entangled tensor network states and report on a variational algorithm to simulate the ground-state physics of many-body systems. We demonstrate that state-of-the-art optical devices are capable of determining the ground-state properties of the spin-1/2 Heisenberg model. Finally, implementations of the scheme are demonstrated to be robust against realistic losses and mode mismatch.

DOI: [10.1103/PhysRevLett.120.130501](https://doi.org/10.1103/PhysRevLett.120.130501)

General quantum states possess a complex entanglement structure that makes their description on a classical computer inefficient in the sense that, generally, the computational effort grows exponentially with the number of subsystems. However, in ground and thermal states of local Hamiltonians, the entanglement and correlations are typically more limited as they satisfy area laws [1–3]. Such states can be approximated well in terms of matrix product states (MPSs) or, more generally, tensor network (TN) states parametrization, in which only a polynomial (in the number of subsystems) number of parameters is required to describe the state [4,5]. This class includes not only the ground states of a wide variety of quantum many-body Hamiltonians [2,6] but also eponymous examples of entangled states such as the Greenberger-Horne-Zeilinger (GHZ) state and  $W$  state. The generation of MPSs is important because they include important resource states for quantum communication, teleportation, and metrology [7–10]. Furthermore, TNs can efficiently parametrize important quantum states, including universal states for quantum computation (e.g., cluster and Affleck-Kennedy-Lieb-Tasaki states [11,12]), states important in high- $T_c$  superconductivity (e.g., resonating valence bond state [13]), and topologically ordered states of matter [14,15]. Although matrix product states can be efficiently manipulated on a classical computer [16], the treatment of TN states in higher spatial dimensions remains challenging because the computational effort, while polynomial, grows with a high power in the number of subsystems and bond dimension. Therefore, the experimental generation of TN states and their use for quantum simulation is of considerable interest.

Current experimental implementations for the generation and processing of TN states focus on spatial modes of light, but these implementations require experimental resources that typically increase quickly with the required size of the

TN state [17–21]. This limitation can be overcome by using the temporal modes of light or time bins, which provide an infinite-dimensional Hilbert space that can be controlled with constant experimental resources through time multiplexing. The potential of this approach has already been successfully demonstrated in the context of quantum walks and boson sampling [22–25]. Existing proposals for generating photonic TN states in the temporal modes of light rely on the strong coupling of light to a single atom trapped inside a cavity [26–28]. The strength of these methods is that they allow the generation of arbitrary 1D TN states whose entanglement is limited only by the number of accessible atomic states. However, the experimental implementation of these schemes requires two challenging conditions to be met, namely, the cooling and localizing of the atom and strong coupling between the atom and the light emitted from the cavity. Moreover, the requirement of complete control over multiple atomic states restricts the amount of entanglement in the generated TN states.

In this Letter, we devise an all-optical scheme for the generation of TN states in one and higher dimensions that overcomes these challenges. Our scheme does not suffer from the stringent requirement of strong atom-photon coupling and instead exploits well established parametric down-conversion (PDC) methods to build entanglement in the generated state [29]. Furthermore, our method overcomes the restriction on entanglement (as quantified by bond dimension) to accessible atomic levels by using the photon-number degree of freedom to share entanglement between components of the generated state. Finally, our all-optical scheme also promises robustness against loss and mode mismatch and can be realized with current optical technology.

*Scheme to generate TN states.*—Our proposed scheme to generate entangled multimode states of light is depicted in Fig. 1. The experimental setup relies on placing a type-II

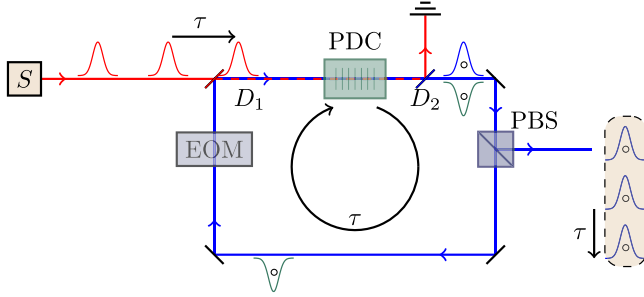


FIG. 1. Setup to generate 1D TN states: the setup includes a PDC nonlinearity placed inside an optical loop. Laser pulses (red) from a source  $S$  placed outside of the loop are fed into it, where they pump the nonlinearity to effect PDC on the two polarization modes of light. One polarization mode (blue) is coupled out of the loop using a PBS. The cycling time  $\tau$  of the signal (green) mode equals the time separation of the pump pulses. Dichroic mirrors  $D_1$  and  $D_2$  couple the pump out. The circles represent superpositions over low-photon-number Fock states. The light modes coupled out from the loop via the PBS contain the desired 1D TN state.

PDC nonlinearity into an optical loop and optically pumping the nonlinearity. This nonlinearity performs two-mode squeezing  $U = \exp(\eta \hat{a}_h^\dagger \hat{a}_v^\dagger - \eta^* \hat{a}_h \hat{a}_v)$  on the horizontal and vertical modes of light, where the PDC parameter  $\eta$  depends on the strength of the optical pumping. Here  $\hat{a}_i^\dagger$  and  $\hat{a}_i$  are the creation and annihilation operators for mode  $i \in \{h, v\}$ . The light in one of the two polarization modes (say, vertical) is coupled out of the loop via a polarizing beam splitter (PBS), while the other (say, horizontal) cycles the loop. An electro-optic modulator (EOM) in the loop dynamically mixes the two polarization modes, of which the vertical mode is in vacuum, via arbitrary linear transformations  $\hat{a}_j^\dagger \rightarrow \sum_{i=1}^2 V_{ij} \hat{a}_i^\dagger$  for  $2 \times 2$  special unitary matrix  $V \in \text{SU}(2)$  [30]. Section A of the Supplemental Material [31] details the modeling of the setup. The time it takes for light to cycle the loop is set equal to the delay between subsequent pump pulses. Thus, the cycling light arrives synchronous to the next pump pulse and effects two-mode squeezing interaction between the two polarization modes [49]. In other words, the PDC and the EOM together give rise to an interaction between the horizontally polarized cycling light and the vertically polarized optical vacuum.

The quantum circuit representing this repeated interaction is presented in Fig. 2. We consider the temporal modes (represented by  $\{\hat{b}_j, \hat{b}_j^\dagger\}$ ) of the light coupled out from the loop over many cycles, where each temporal mode is the vertically polarized mode that was coupled out from the PBS at a different time. We show the establishment of multiparticle entanglement between subsequent temporal modes mediated by the light cycling in the loop as depicted by the dashed line of Fig. 2. Specifically, we show that the emitted temporal modes of light permit a 1D TN representation and include entangled states such as  $W$  and GHZ

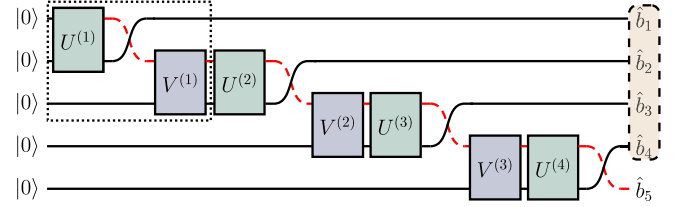


FIG. 2. Quantum circuit of 1D experiment for four cycles.  $U^{(i)}$  represents the two-mode PDC process and  $V^{(i)}$  represents the EOM transformation in the  $i$ th cycle. The dotted box represents one cycle. The action of the PBS is represented by the mode swapping after each  $U^{(i)}$  operation and a subsequent emission of one of the polarization modes. The red dashed line represents the cycling mode. The rounded box on the right encloses subsequently emitted temporal modes  $\{\hat{b}_j\}$  that contain the state of interest.

states. The proof for this result and the general form of the resultant TN state is in the Supplemental Material, Sec. B [31]. The intuition for the proof is that the cycling mode mediates entanglement between subsequently emitted light modes. Entanglement between one emitted mode and the next is limited by the entanglement between the first mode and the cycling mode, and this maximum entanglement is constant, irrespective of the number of cycles. Because subsequent temporal modes of light are entangled, albeit with limited entanglement, it follows that the state of the emitted light can be represented as a TN state of limited bond dimension.

Although the properties of 1D TN states can be efficiently obtained on a classical computer, those of TN states in two and higher dimensions require classical algorithms that scale badly, i.e., exponentially in the system size and as high-degree polynomials in the bond dimension. In other words, two- and higher-dimensional TN states can be exploited for obtaining nontrivial quantum-computational speed up. It is possible to modify our scheme to generate higher-dimensional TN states by connecting additional optical loops into the existing loop, as depicted in Fig. 3. The effect of one additional loop is to convert different polarization modes into temporal modes, an approach already used in 2D quantum walks [22,50]. Optionally, additional nonlinearities and EOMs can be added to the loop to ensure that the entanglement structure is identical in the two dimensions of the lattice. The additional optical loop is designed to provide a time delay of  $\tau/n$ , which is smaller than the cycling time  $\tau$  of the main loop by a factor  $n$  for some large integer  $n$ . Owing to this additional time delay, the difference between the emission times of two temporal modes is either  $\tau$  or multiples  $\tau/n$ ,  $2\tau/n$ ,  $3\tau/n$ , ... of the interval  $\tau/n$ . Modes with time difference  $\tau$  are interpreted as neighbors along one axis of the TN lattice, whereas those with time difference  $\tau/n$  are interpreted as neighbors along a different axis. Depending on the required number  $\tilde{n}$  of lattice sites along the second TN dimension, we can choose any  $n > \tilde{n}$  so that the sites in the 2D lattice are uniquely defined. Thus, the emitted light

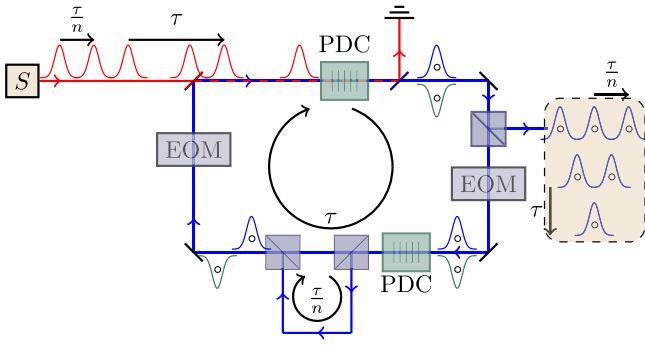


FIG. 3. Setup to generate 2D TN states: to generate 2D TN states, an additional fiber loop (corresponding to a time delay  $\tau/n$  for chosen integer  $n$ ) is connected into the existing 1D loop via PBSs. Pumping of the additional optional PDC is omitted from the figure for simplicity. TN states in more than two dimensions can be generated by introducing additional fiber loops into the optical setup.

possesses an entanglement structure that is captured by a 2D TN state with a triangular structure (see Supplemental Material, Sec. B [31]). Similarly, additional loops can be connected to the optical setup to generate higher-dimensional TN states. We estimate that current optical technology can enable the generation of five-mode 1D TN states and 15-mode 2D TN states at the rates of 1200 and 85 Hz, respectively (Supplemental Material, Sec. E [31]).

*State generation.*—Here we detail how the setup can be used to generate two inequivalent classes of entangled states, namely, the  $W$  and GHZ states. First, we consider the  $m$ -qubit  $W$  state  $|\psi\rangle_W = |0\dots 01\rangle + |0\dots 10\rangle + \dots + |1\dots 00\rangle$ , which has one excitation  $|1\rangle$  that is delocalized uniformly over all the qubits. Our proposed setup can generate a heralded  $W$  state, which is defined as

$$|\psi\rangle_{HW} = |0\dots 00\rangle \otimes |0\rangle + \eta(|0\dots 01\rangle + |0\dots 10\rangle + \dots + |1\dots 00\rangle) \otimes |1\rangle \quad (1)$$

on a total of  $m + 1$  qubits for some complex  $\eta$  with  $\eta < 1$  and the normalization factor is omitted for simplicity. In this state, a  $|1\rangle$  in the last qubit heralds the presence of a  $W$  state in the remaining qubits, whereas a  $|0\rangle$  in the last qubit implies a vacuum state in the remaining qubits.

The heralded  $W$  state can be generated by our proposed setup in the single-rail basis [51], wherein the absence of a photon in a temporal mode encodes the state  $|0\rangle$  and a single photon in the mode encodes  $|1\rangle$ . Cases where more than a single photon is present in the mode are discarded. Even after accounting for this postselection, high rates of state generation on the order of kilohertz can be obtained (Supplemental Material, Sec. E [31]).

Next we describe the generation of the 4-qubit GHZ state [52], which is usually defined as an equal superposition  $|0000\rangle + |1111\rangle$  over each qubit that is in state  $|0\rangle$  and each qubit in state  $|1\rangle$ . An alternative description of the GHZ

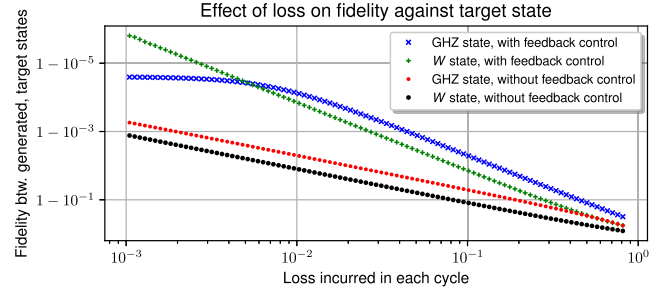


FIG. 4. Simulations: effect of loss on the fidelity of the generated 4-qubit state with respect to target  $W$  and GHZ states. The red and black dots represent the fidelity between the respective generated and target state as a function of the loss incurred by the light in each cycle. The blue and green crosses represent the same quantity under self-correction, i.e., when variational algorithms are used to find circuit parameters that optimize the fidelity against the target state in the lossy case.

state  $|1100\rangle + |0011\rangle$  is obtained by redefining the qubit labels in the last two qubits. Our proposed setup can be used to generate the diluted GHZ state

$$|\psi\rangle_{\text{GHZ}} = |0000\rangle + \eta(|0011\rangle + |1100\rangle), \quad (2)$$

where the normalization factor is omitted. Supplemental Material Sec. C details the optical circuit parameters for generating these states [31].

In both cases of heralded  $W$ - and diluted GHZ-state generation, we can obtain experimental results for  $W$  and GHZ states by postselecting only those experimental outcomes in which the expected numbers of photons were observed. Simulations provide evidence that our state generation procedure is robust against the usual experimental imperfections of loss and mode mismatch from the PDC. Consider reasonable experimental losses, which are typically upward of 10% loss in each cycle; these losses can lead to higher than 90% fidelity with respect to target state, as seen in the red and black dots of Fig. 4.

*Quantum-variational algorithm.*—Other than state preparation, the proposed setup can be exploited for performing a mixed quantum-classical algorithm for the determination of ground-state properties of many-body systems via a quantum-variational approach, which we now describe. We consider the task of determining the properties, such as the energy or correlations, of the ground state of a given Hamiltonian operator that acts on qubits. The generated TN states comprise the set of variational states; their energy with respect to the given Hamiltonian is obtained by performing Glauber correlation measurements on the output light following the procedure of [53] in single-rail representation [54,55]. A classical minimization algorithm can then be used to obtain circuit parameters corresponding to the generated state that has the lowest energy with respect to the given Hamiltonian. If the circuit parameters, including the pump strength and EOM

parameters, are sufficiently expressive, i.e., if the ground state is close to the class of variational states generated by the setup, then an accurate approximation of the given Hamiltonian's ground state can be obtained. The procedure is expected to work well for a wide variety of Hamiltonians because the ground state of most 1D local Hamiltonians is close to a low-dimension TN state [2]. The properties of the ground state can be determined by usual measurements on the output light. Our mixed quantum-classical variational approach encompasses the variational problem that can be solved using the so-called Ising machines because it exploits the polarization and photon-number degrees of freedom in addition to temporal modes used in Ising machines [56,57].

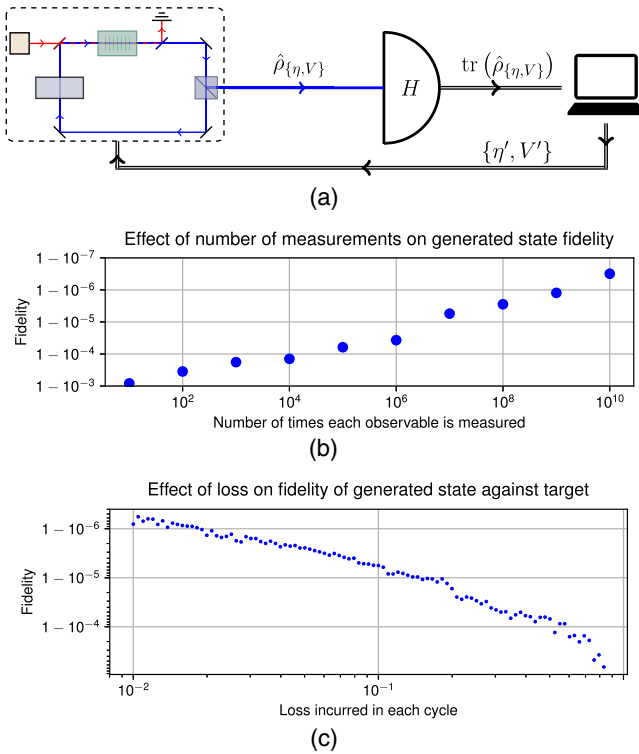


FIG. 5. (a) Scheme of quantum-variational algorithm and simulated performance under (b) finite numbers of measurements and (c) losses. (a) Depiction of quantum-variational algorithm. The output from the setup (parameters set to  $\{\eta\}, \{V\}$ ) is fed into detection setup that encodes the given Hamiltonian  $H$ . The detector output is analyzed by a classical optimization routine to choose the set of variational parameters  $\{\eta'\}, \{V'\}$  for the next step. (b) The simulated number of measurements performed for each observable versus the fidelity  $F$  between the expected ground state ( $W$  state) and the state obtained from the quantum-variational algorithm, without including the effect of losses. (c) The fidelity between the expected ground state and the state obtained from the quantum-variational algorithms as a function of simulated loss in each loop. The variational algorithm chooses a different pumping value for each cycle. See Supplemental Material, Sec. D for simulation details and Sec. E for experimental considerations [31].

To illustrate the performance of this approach, we simulate the procedure to find the ground state of the isotropic XY model [58,59]. The ground state of the XY Hamiltonian  $H_{XY} = J\sum_i X_i X_{i+1} + Y_i Y_{i+1} + (B/4)\sum_i Z_i$  is the  $W$  state for a certain range of  $B$  [60]. We simulate Glauber correlation measurements on the output light to obtain the energy of the generated state for a specific value of circuit parameters [53]. Starting with random circuit parameters, we use a constrained minimization algorithm to find those circuit parameters that minimize the energy. The variational minimization returns a state that is close to the expected ground state, as depicted in Fig. 5. Simulations provide evidence that this approach is robust against statistical noise [Fig. 5(b)] and loss [Fig. 5(c)].

A similar variational approach can also be used to enhance the quality of state generation, as described above, against possible experimental imperfections. For instance, consider the task of improving the fidelity  $F = \langle \psi_t | \rho_{\text{lab}} | \psi_t \rangle$  of the generated state  $\rho_{\text{lab}}$  with respect to a given target state  $|\psi_t\rangle$ , such as the  $W$  state, under the presence of imperfections such as loss and phase drift. We can leverage from a measurement-based feedback control scheme [61] to find the circuit parameters that maximize fidelity against a desired state and thereby compensate for experimental imperfections. Direct fidelity estimation procedures [62,63] can be used to efficiently estimate the fidelity with respect to the desired state and classical optimization can be performed to maximize this fidelity. Simulations show that our  $W$  and GHZ state generation procedures can be made further resilient to loss via such feedback control by 2–3 orders of magnitude (see blue and green crosses in Fig. 4).

*Discussion.*—In summary, we propose a scheme for the all-optical generation of one- and higher-dimensional TN states in temporal modes of light. The free parameters describing the TN state and its bond dimension can be improved by using additional degrees of freedom of light, such as spatial modes, time-frequency Schmidt modes, and orbital angular momentum modes of light [64–67], or by adding another EOM to the loop between the PDC and the PBS. Finally, states such as coherent states can be impinged into the PDC instead of starting with the optical vacuum, thereby leading to the generation of high-photon-number Gaussian matrix product states [68,69], which could potentially be used as a resource for Gaussian boson sampling [70,71]. Efficient TN-based procedures can be employed to perform tomography of the states [72–75].

We thank Raul Garcia-Patron, Sandeep K. Goyal, Milan Holzäpfel, W. Steven Kolthammer, Leonardo Novo, and Johannes Tiedau for helpful discussions. We acknowledge support by the state of Baden-Württemberg through bwHPC and the German Research Foundation (DFG) through Grant No. INST 40/467-1 FUGG. The group at Ulm was supported by the ERC Synergy Grant BioQ, the EU project QUCHIP, and by the Alexander von Humboldt Foundation via the Humboldt Research Fellowship for

Postdoctoral Researchers. The group at Paderborn acknowledges financial support from the Gottfried Wilhelm Leibniz-Preis (Grant No. SII115/3-1), from the European Union's Horizon 2020 research and innovation program under the QUCHIP project GA No. 641039, and from European Commission with the ERC project QuPoPCoRN (No. 725366).

*Note added.*—Please see the related paper [48] that has been recently listed by Lubasch *et al.*

- 
- [1] K. Audenaert, J. Eisert, M. B. Plenio, and R. F. Werner, *Phys. Rev. A* **66**, 042327 (2002).
- [2] J. Eisert, M. Cramer, and M. B. Plenio, *Rev. Mod. Phys.* **82**, 277 (2010).
- [3] F. G. S. L. Brandão and M. Horodecki, *Commun. Math. Phys.* **333**, 761 (2015).
- [4] R. Orús, *Ann. Phys. (Amsterdam)* **349**, 117 (2014).
- [5] F. Verstraete, V. Murg, and J. Cirac, *Adv. Phys.* **57**, 143 (2008).
- [6] N. Schuch, M. M. Wolf, F. Verstraete, and J. I. Cirac, *Phys. Rev. Lett.* **100**, 030504 (2008).
- [7] C. Wang, F. G. Deng, and G. L. Long, *Opt. Commun.* **253**, 15 (2005).
- [8] Z.-L. Cao and W. Song, *Physica (Amsterdam)* **347A**, 177 (2005).
- [9] W. Jian, Z. Quan, and T. Chao-Jing, *Commun. Theor. Phys.* **48**, 637 (2007).
- [10] M. Jarzyna and R. Demkowicz-Dobrzański, *Phys. Rev. Lett.* **110**, 240405 (2013).
- [11] R. Raussendorf and H. J. Briegel, *Phys. Rev. Lett.* **86**, 5188 (2001).
- [12] T.-C. Wei, I. Affleck, and R. Raussendorf, *Phys. Rev. Lett.* **106**, 070501 (2011).
- [13] P. W. Anderson, *Science* **235**, 1196 (1987).
- [14] A. Kitaev, *Ann. Phys. (Amsterdam)* **303**, 2 (2003).
- [15] F. Verstraete, M. M. Wolf, D. Perez-Garcia, and J. I. Cirac, *Phys. Rev. Lett.* **96**, 220601 (2006).
- [16] U. Schollwöck, *Ann. Phys. (Amsterdam)* **326**, 96 (2011).
- [17] X. B. Zou, K. Pahlke, and W. Mathis, *Phys. Rev. A* **66**, 044302 (2002).
- [18] X. B. Zou and W. Mathis, *Phys. Rev. A* **71**, 032308 (2005).
- [19] X. Su, A. Tan, X. Jia, J. Zhang, C. Xie, and K. Peng, *Phys. Rev. Lett.* **98**, 070502 (2007).
- [20] M. Yukawa, R. Ukai, P. van Loock, and A. Furusawa, *Phys. Rev. A* **78**, 012301 (2008).
- [21] Y.-F. Huang, B.-H. Liu, L. Peng, Y.-H. Li, L. Li, C.-F. Li, and G.-C. Guo, *Nat. Commun.* **2**, 546 (2011).
- [22] A. Schreiber, K. N. Cassemiro, V. Potoček, A. Gábris, P. J. Mosley, E. Andersson, I. Jex, and C. Silberhorn, *Phys. Rev. Lett.* **104**, 050502 (2010).
- [23] A. Schreiber, K. N. Cassemiro, V. Potoček, A. Gábris, I. Jex, and C. Silberhorn, *Phys. Rev. Lett.* **106**, 180403 (2011).
- [24] K. R. Motes, A. Gilchrist, J. P. Dowling, and P. P. Rohde, *Phys. Rev. Lett.* **113**, 120501 (2014).
- [25] Y. He *et al.*, *Phys. Rev. Lett.* **118**, 190501 (2017).
- [26] C. Schön, E. Solano, F. Verstraete, J. I. Cirac, and M. M. Wolf, *Phys. Rev. Lett.* **95**, 110503 (2005).
- [27] C. Schön, K. Hammerer, M. M. Wolf, J. I. Cirac, and E. Solano, *Phys. Rev. A* **75**, 032311 (2007).
- [28] H. Pichler, S. Choi, P. Zoller, and M. D. Lukin, *Proc. Natl. Acad. Sci. U.S.A.* **114**, 11362 (2017).
- [29] L.-A. Wu, H. J. Kimble, J. L. Hall, and H. Wu, *Phys. Rev. Lett.* **57**, 2520 (1986).
- [30] J. Capmany and C. Fernández-Pousa, *Laser Photonics Rev.* **5**, 750 (2011).
- [31] See Supplemental Material at <http://link.aps.org/supplemental/10.1103/PhysRevLett.120.130501> for details about setup modelling, main proof, generation of  $W$  and GHZ states, simulations and experimental considerations, which includes Refs. [32–48].
- [32] D. Achilles, C. Silberhorn, C. Šliwa, K. Banaszek, and I. A. Walmsley, *Opt. Lett.* **28**, 2387 (2003).
- [33] M. Avenhaus, M. V. Chekhova, L. A. Krivitsky, G. Leuchs, and C. Silberhorn, *Phys. Rev. A* **79**, 043836 (2009).
- [34] K. Banaszek and I. A. Walmsley, *Opt. Lett.* **28**, 52 (2003).
- [35] A. Christ, K. Laiho, A. Eckstein, K. N. Cassemiro, and C. Silberhorn, *New J. Phys.* **13**, 033027 (2011).
- [36] W. Dür, G. Vidal, and J. I. Cirac, *Phys. Rev. A* **62**, 062314 (2000).
- [37] T. Gerrits, A. Lita, B. Calkins, and S. W. Nam, in *Superconducting Devices in Quantum Optics*, edited by R. H. Hadfield and G. Johansson (Springer International Publishing, Cham, 2016) p. 31.
- [38] W. P. Grice and I. A. Walmsley, *Phys. Rev. A* **56**, 1627 (1997).
- [39] G. Harder, V. Ansari, B. Brecht, T. Dirmeier, C. Marquardt, and C. Silberhorn, *Opt. Express* **21**, 13975 (2013).
- [40] J. Johansson, P. Nation, and F. Nori, *Comput. Phys. Commun.* **183**, 1760 (2012).
- [41] T. E. Keller and M. H. Rubin, *Phys. Rev. A* **56**, 1534 (1997).
- [42] F. Marsili, V. B. Verma, J. A. Stern, S. Harrington, A. E. Lita, T. Gerrits, I. Vayshenker, B. Baek, M. D. Shaw, R. P. Mirin *et al.*, *Nat. Photonics* **7**, 210 (2013).
- [43] D. Perez-Garcia, F. Verstraete, M. M. Wolf, and J. I. Cirac, *Quantum Inf. Comput.* **7**, 401 (2007).
- [44] R. E. Perez, P. W. Jansen, and J. R. Martins, *Struct. Multidiscip. Optim.* **45**, 101 (2012).
- [45] M. J. D. Powell, in *Numerical Analysis: Proceedings of the Biennial Conference Held at Dundee, 1977*, edited by G. A. Watson (Springer, Berlin, 1978) p. 144.
- [46] D. Rosenberg, A. E. Lita, A. J. Miller, and S. W. Nam, *Phys. Rev. A* **71**, 061803 (2005).
- [47] D. Suess and M. Holzäpfel, *J. Open Source Software* **2**, 465 (2017).
- [48] M. Lubasch, A. A. Valido, J. J. Renema, W. S. Kolthammer, D. Jaksch, M. S. Kim, I. Walmsley, and R. García-Patrón, [arXiv:1712.09869](https://arxiv.org/abs/1712.09869).
- [49] C. Simon, G. Weihs, and A. Zeilinger, *Phys. Rev. Lett.* **84**, 2993 (2000).
- [50] A. Schreiber, A. Gábris, P. P. Rohde, K. Laiho, M. Štefaňák, V. Potoček, C. Hamilton, I. Jex, and C. Silberhorn, *Science* **336**, 55 (2012).
- [51] T. C. Ralph and G. J. Pryde, *Prog. Opt.* **54**, 209 (2010).
- [52] D. M. Greenberger, M. A. Horne, and A. Zeilinger, in *Bell's Theorem, Quantum Theory and Conceptions of the Universe*, edited by M. Kafatos (Springer, Dordrecht, 1989) p. 69.

- [53] S. Barrett, K. Hammerer, S. Harrison, T. E. Northup, and T. J. Osborne, *Phys. Rev. Lett.* **110**, 090501 (2013).
- [54] A. P. Lund and T. C. Ralph, *Phys. Rev. A* **66**, 032307 (2002).
- [55] G. Donati, T. J. Bartley, X.-M. J. Mihai-Dorian Vidrighin, A. Datta, M. Barbieri, and I. A. Walmsley, *Nat. Commun.* **5**, 5584 (2014).
- [56] P. L. McMahon, A. Marandi, Y. Haribara, R. Hamerly, C. Langrock, S. Tamate, T. Inagaki, H. Takesue, S. Utsunomiya, K. Aihara, R. L. Byer, M. M. Fejer, H. Mabuchi, and Y. Yamamoto, *Science* **354**, 614 (2016).
- [57] W. R. Clements, J. J. Renema, Y. H. Wen, H. M. Chrzanowski, W. S. Kolthammer, and I. A. Walmsley, *Phys. Rev. A* **96**, 043850 (2017).
- [58] E. Lieb, T. Schultz, and D. Mattis, *Ann. Phys. (N.Y.)* **16**, 407 (1961).
- [59] M. Takahashi, *Thermodynamics of One-Dimensional Solvable Models* (Cambridge University Press, Cambridge, 2005), p. 1, DOI: [10.1017/CBO9780511524332](https://doi.org/10.1017/CBO9780511524332).
- [60] T. Zhang, P.-X. Chen, W.-T. Liu, and C.-Z. Li, [arXiv: 1206.4246](https://arxiv.org/abs/1206.4246).
- [61] R. Inoue, S.-I.-R. Tanaka, R. Namiki, T. Sagawa, and Y. Takahashi, *Phys. Rev. Lett.* **110**, 163602 (2013).
- [62] S. T. Flammia and Y.-K. Liu, *Phys. Rev. Lett.* **106**, 230501 (2011).
- [63] M. P. da Silva, O. Landon-Cardinal, and D. Poulin, *Phys. Rev. Lett.* **107**, 210404 (2011).
- [64] M. Reck, A. Zeilinger, H. J. Bernstein, and P. Bertani, *Phys. Rev. Lett.* **73**, 58 (1994).
- [65] L. Marrucci, E. Karimi, S. Slussarenko, B. Piccirillo, E. Santamato, E. Nagali, and F. Sciarrino, *J. Opt.* **13**, 064001 (2011).
- [66] B. Brecht, D. V. Reddy, C. Silberhorn, and M. G. Raymer, *Phys. Rev. X* **5**, 041017 (2015).
- [67] I. Dhand and S. K. Goyal, *Phys. Rev. A* **92**, 043813 (2015).
- [68] C. C. Gerry, *J. Mod. Opt.* **42**, 585 (1995).
- [69] N. Schuch, M. M. Wolf, and J. I. Cirac, in *Quantum Information and Many Body Quantum Systems: Proceedings*, edited by M. Ericsson and S. Montangero, CRM Series (Edizioni della Normale, Pisa, 2008) p. 129.
- [70] C. S. Hamilton, R. Kruse, L. Sansoni, S. Barkhofen, C. Silberhorn, and I. Jex, *Phys. Rev. Lett.* **119**, 170501 (2017).
- [71] L. Chakhmakhchyan and N. J. Cerf, *Phys. Rev. A* **96**, 032326 (2017).
- [72] M. Cramer, M. B. Plenio, S. T. Flammia, R. Somma, D. Gross, S. D. Bartlett, O. Landon-Cardinal, D. Poulin, and Y.-K. Liu, *Nat. Commun.* **1**, 149 (2010).
- [73] T. Baumgratz, A. Nüßeler, M. Cramer, and M. B. Plenio, *New J. Phys.* **15**, 125004 (2013).
- [74] T. Baumgratz, D. Gross, M. Cramer, and M. B. Plenio, *Phys. Rev. Lett.* **111**, 020401 (2013).
- [75] B. P. Lanyon, C. Maier, M. Holzäpfel, T. Baumgratz, C. Hempel, P. Jurcevic, I. Dhand, A. S. Buyskikh, A. J. Daley, M. Cramer, M. B. Plenio, R. Blatt, and C. F. Roos, *Nat. Phys.* **13**, 1158 (2017).